Chapter 4
Discontinuous Approach to Concrete

Abstract. The Chapter discusses discontinuous approaches to simulate cracks in concrete. Two approaches are described: a cohesive crack model using interface elements defined along finite element boundaries and eXtended Finite Element Method (XFEM) wherein cracks can occur arbitrarily in the interior of finite elements.

4.1 Cohesive Crack Model

A cohesive crack model for simulating macro-cracks as discontinuities was initiated from the Hilleborg's fictitious crack model (Hilleborg et al. 1976) based on the idea of Dugdale (1960) and was further applied in conjunction with interface elements (cohesive elements) by Camacho and Ortiz (1996). No information on an initial crack needs to be known and the onset of crack initiation can be predicted within a preset cohesive zone, which is considered to be a potential crack propagation path. The cohesive crack model describes highly localized inelastic processes by traction-separation laws that link the cohesive traction transmitted by a discontinuity or surface to the displacement jump characterized by the separation vector (Needleman 1987, Camacho and Ortiz 1996, Ortiz and Pandolfi 1999, Chandra et al. 2002, Gálvez et al. 2002, Scheider and Brocks 2003, Zhou and Molinari 2004, de Lorenzis and Zavarise 2009). Cohesive elements are defined at the edges (interface) between standard finite elements to nucleate cracks and propagate them following the deformation process. They govern the separation of crack flanks in accordance with an irreversible cohesive law. Branching, crack coalescence, kinking and tortuousness (any material separation) are naturally handled by this approach. If the crack path is not known a priori, cohesive surfaces are placed between all finite elements. Interfacial normal and tangential tractions are non-linearly connected to the normal (mode-I) and tangential (mode-II) relative displacements on the interface. As the cohesive interface gradually separates, the magnitude of interfacial stresses at first increases, reaches a maximum, and then decreases with increasing separation, finally approaching zero. Thus, depending on the level of the interfacial relative displacements, the cohesive interface represents

J. Tejchman, J. Bobiński: Continuous & Discontinuous Modelling of Fracture, SSGG, pp. 95–107.
springerlink.com

the entire spectrum of the behaviour ranging from perfect bonding to complete separation. A shape of post-peak traction-opening is linked with the development of the so-called fracture process zone where many complex phenomena occur such as micro-cracking, interlocking, bridging, friction between surfaces and aggregates, etc. The fundamental material parameters in cohesive models for concrete are the fracture energy and the shape of the traction versus crack opening. The cohesive fracture energy is the external energy required to create and fully break a unit surface area of a cohesive crack and coincides with the area under the softening function. The crack models can be based on formulations of the classical plasticity (Gálvez et al. 2002) or damage mechanics (Omiya and Kishimoto 2010). The model is attractive since it is straightforward in implementation.

The cohesive crack model provides an objective description of fully localized failure if the mesh is fine. The cohesive traction-separation law with softening does not need any adjustment for the element size because mesh refinement does not change the resolved crack pattern. However, the model possesses some restrictions. The crack paths are dominated by preferred mesh orientations (Zhou and Molinari 2004) and the mesh independence is questionable if the cracking pattern is diffuse (Bažant and Jirásek 2002). Moreover, stress multiaxiality in the fracture process zone is not captured (Bažant and Jirásek 2002). In models with interface elements inserted a priori, spurious elastic deformation occurs prior to cracking onset, so too high initial elastic normal stiffness can lead to spurious traction oscillations in the pre-cracking phase (de Borst and Remmers 2006). A dummy stiffness (theoretically infinite) is usually required to keep the inactive interface elements closed. The mesh dependency can be improved if the mesh is very fine, inertia forces and viscosity are included, a non-local formulation for the interface mode is used, a separation approximation in the process zone is enriched (de Borst and Remmers 2006, Samimi et al. 2009) or cohesive elements strength follows a stochastic distribution (Zhou and Molinari 2004, Yang and Xu 2008). Recently, Cazes et al. (2009) proposed a thermodynamic method for the construction of a cohesive law from a nonlocal damage model.

The cohesive zone model includes 3 main steps:

- the constitutive continuum modelling (usually by means of linear elasticity if tensile loading prevails),
- the introduction of an initiation criterion for crack opening/growth (loading function),
- the evolution equation for softening of normal/shear tractions.

To take into account mixed mode loading conditions Camacho and Ortiz (1996) defined the effective crack opening displacement as

$$\delta_{eff} = \sqrt{\delta_n^2 + \eta^2 \delta_s^2} \,, \tag{4.1}$$

wherein δ_n and δ_s are the normal crack opening displacement and tangential relative displacement (sliding), respectively, while the coefficient η takes into

account the coupling between the failure mode I and failure mode II. The loading function is defined as

$$f\left(\delta_{eff},\kappa\right)=\delta_{eff}-\kappa \tag{4.2}$$

with the history parameter κ equal to the maximum value of the effective displacement δ_{eff} obtained during loading. The effective traction is

$$t_{eff}=\sqrt{t_n^2+\eta^{-2}t_s^2}\ . \tag{4.3}$$

The effective traction t_{eff} is calculated with the aid of an exponential, bilinear or linear softening relationship. Finally, the normal and shear tractions are evaluated as

$$t_n=\frac{t_{eff}}{\delta_{eff}}\delta_n \qquad \text{and} \qquad t_s=\eta^2\frac{t_{eff}}{\delta_{eff}}\delta_s\ . \tag{4.4}$$

Unloading takes place to the origin. In compression, the penalty stiffness is applied.

We used a simple version of a cohesive crack model with interface elements placed 'a priori' between all finite elements of the FE mesh (Fig. 4.1). The bulk finite elements were modeled as linear elastic. In turn, in the interface elements, a damage constitutive relationship between the traction vector $\boldsymbol{t}=[t_n,\ t_s]$ and relative displacement vector $\boldsymbol{\delta}=[\delta_n,\ \delta_s]$ was assumed

$$t=\left(1-D\right)E_0\boldsymbol{I}\boldsymbol{\delta} \tag{4.5}$$

with the penalty (dummy) stiffness E_0 and unit tensor $\boldsymbol{I}$. To take into account both the normal and shear terms in the separation vector, an effective opening displacement was used by Eq. 4.1. To describe softening after cracking, an exponential law was assumed following Camacho and Ortiz (1996)

$$t_{eff}\left(\kappa\right)=f_t\exp\left(-\beta\left(\kappa-\frac{f_t}{E_0}\right)\right), \tag{4.6}$$

where β is the model parameter. The crack was initiated if (Fig. 4.2)

$$\kappa=\delta_0=\frac{f_t}{E_0}\ . \tag{4.7}$$

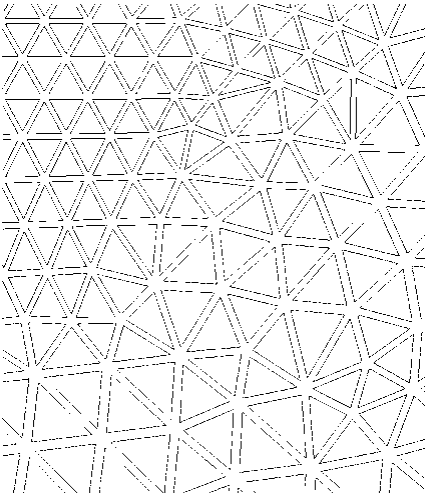

Fig. 4.1 Bulk and cohesive (interface) elements in FE mesh (Bobiński and Tejchman 2008)

The damage parameter was equal to

$$D = 1 - \frac{1}{E_0}\frac{t_{eff}}{\delta_{eff}}. \tag{4.8}$$

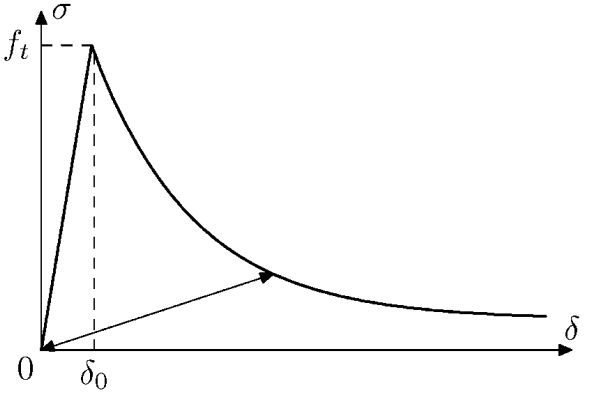

Fig. 4.2 Traction-separation cohesive law assumed for numerical calculations (Bobiński and Tejchman 2008)

4.2 Extended Finite Element Method

The Extended Finite Element Method (XFEM) is based on the Partition of Unity concept (Melenk and Babuska 1996) that allows for adding locally extra terms to

the standard FE displacement field approximation in order to capture displacement discontinuities. These extra terms are defined based on a known analytical solution of the problem. The idea is to enrich only selected nodes with additional terms. There is no need to modify the original FE mesh (Belytschko and Black 1999) used to model cracks in elastic-brittle materials. To describe the stress field around the crack tip, Moes and Belytschko (1999) formulated a model with branch functions for elements with crack tip and Heaviside jump function for elements cut entirely by a crack. Later XFEM was extended to deal with branching and intersecting cracks (Daux et al. 2000) and to simulate three-dimensional problems (Sukumar et al. 2000). In turn, Samaniego and Belytschko (2005) simulated dynamic propagation of shear zones. The enrichment was defined only in tangential direction and no separation was allowed in normal direction. XFEM was also used to analyze problems with weak discontinuities (like material interfaces), and in fluid mechanics by modelling voids and holes, phase transformations, biofilms and dislocations. Wells and Sluys (2001) were the first to couple XFEM with cohesive cracks (only Heaviside jump function was defined to describe the displacement jump across the discontinuity). Moes and Belytschko (2002) used XFEM to simulate cohesive cracks. Zi and Belytschko (2003) formulated a new crack tip element using linear ramp functions for the description of the crack tip location. Mergheim et al. (2005) adopted the idea of Hansbo and Hansbo (2004) with no extra degrees of freedom in nodes. Any element with a crack was described by two overlapping standard finite elements with zero shape functions either on the left and on the right side of a discontinuity. Only displacement degrees of freedom were used, but extra phantom nodes had to be added in cracked elements to double standard nodes at the moment of cracking. This phantom node method turned out to be equivalent with the XFEM method. This approach later has been used by Song et al. (2006) to simulate cohesive shear zones. Rabczuk et al. (2008) extended the phantom node method for handling crack tips also inside of elements. To simulate shear zones in soils, a discrete Mohr-Coulomb law with softening was used by Bobiński and Brinkgreve (2010).

The formulation used here follows (with some minor modifications) the original model proposed by Wells and Sluys (2001). In a body Ω crossed by a discontinuity Γ_u (Fig. 4.3), a displacement field $\boldsymbol{u}$ can be decomposed into a continuous part $\boldsymbol{u}_{cont}$ and discontinuous part $\boldsymbol{u}_{disc}$. A displacement field can be defined as (Belytschko and Black 1999, Wells and Sluys 2001)

$$\boldsymbol{u}(\boldsymbol{x},t) = \hat{\boldsymbol{u}}(\boldsymbol{x},t) + \Psi(\boldsymbol{x})\tilde{\boldsymbol{u}}(\boldsymbol{x},t) \tag{4.9}$$

with the continuous functions $\hat{u}$ and $\tilde{u}$ and the generalized step function Ψ

$$\Psi(\boldsymbol{x}) = \begin{cases} 1 & \boldsymbol{x} \in \Omega^+ \\ -1 & \boldsymbol{x} \in \Omega^- \end{cases}. \tag{4.10}$$

Other definitions can be also used here, e.g. the Heaviside step function. A collection of functions ϕ_i associated with set of discrete points i (i=1, 2, …, n) constitutes the partition of unity if

$$\sum_{i=1}^{n} \phi_i(\boldsymbol{x}) = 1, \qquad \forall \boldsymbol{x} \in \Omega. \tag{4.11}$$

A field $\boldsymbol{u}$ over body Ω can be interpolated as

$$\boldsymbol{u} = \sum_{i=1}^{n} \phi_i \left(a_i + \sum_{i=1}^{m} b_{ij} \gamma_j \right), \tag{4.12}$$

where a_i and b_{ij} are the discrete nodal values, γ_j – the enhanced basis and m – the number of enhanced terms for a particular node. The finite element shape functions N_i also define the partition of unity concept since

$$\sum_{i=1}^{n} N_i(\boldsymbol{x}) = 1, \qquad \forall \boldsymbol{x} \in \Omega. \tag{4.13}$$

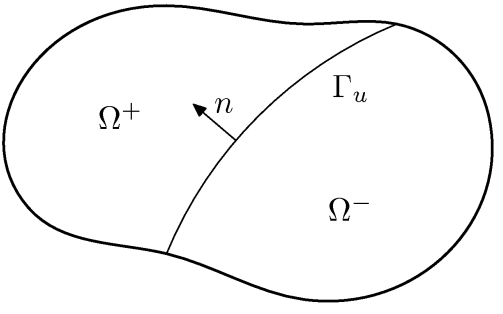

Fig. 4.3 Body crossed by a discontinuity

In a finite element format, Eq. 4.9 can be written as

$$\boldsymbol{u}(\boldsymbol{x}) = \boldsymbol{N}(\boldsymbol{x})\boldsymbol{a} + \boldsymbol{\Psi}(\boldsymbol{x})\boldsymbol{N}(\boldsymbol{x})\boldsymbol{b}, \tag{4.14}$$

where $\boldsymbol{N}$ contains shape functions, $\boldsymbol{a}$ – standard displacements at nodes and $\boldsymbol{b}$ – enriched displacements (jumps) at nodes. Only nodes belonging to 'cracked' elements are enriched. Here a formulation by Belytschko et al. (2001) called the shifted-basis enrichment is used that assumes the following definition of the displacement field

$$\boldsymbol{u}(\boldsymbol{x}) = \boldsymbol{N}(\boldsymbol{x})\boldsymbol{a} + \left(\boldsymbol{\Psi}(\boldsymbol{x}) - \boldsymbol{\Psi}(\boldsymbol{x}_I)\right)\boldsymbol{N}(\boldsymbol{x})\boldsymbol{b} \tag{4.15}$$

with the diagonal matrices $\boldsymbol{\Psi}(\boldsymbol{x})$ and $\boldsymbol{\Psi}(\boldsymbol{x}_I)$ containing $\boldsymbol{\Psi}(\boldsymbol{x})$ and $\boldsymbol{\Psi}(\boldsymbol{x}_I)$, respectively ($\boldsymbol{x}_I$ is the position of the node *I*). The strain rate in the bulk continuum can be calculated as

$$\dot{\boldsymbol{\varepsilon}} = \boldsymbol{B}\dot{\boldsymbol{a}} + \left(\boldsymbol{\Psi} - \boldsymbol{\Psi}_I\right)\boldsymbol{B}\dot{\boldsymbol{b}}\,, \tag{4.16}$$

whereas the rate of the displacement jump $[[\boldsymbol{u}]]$ at the discontinuity is defined as

$$[[\dot{\boldsymbol{u}}]] = 2\boldsymbol{N}\dot{\boldsymbol{b}}\,. \tag{4.17}$$

This formulation has two main advantages over the standard version (Eq. 4.9); the total displacements in nodes are equal to the standard displacements $\boldsymbol{a}$ and the implementation is simpler since two types of elements exist only.

The weak form of the equilibrium equation

$$\int_\Omega \nabla^s \boldsymbol{\eta} : \boldsymbol{\sigma}\,\mathrm{d}\Omega - \int_{\Gamma_u} \boldsymbol{\eta}\cdot\bar{\boldsymbol{t}}\,\mathrm{d}\Gamma = 0 \tag{4.18}$$

holds for all admissible displacement variations η (body forces are neglected and $\bar{t}$ stands for tractions applied on the boundary Γ_u). After several transformations (Wells 2001, Bobiński and Brinkgreve 2010), the following discrete weak equations are obtained

$$\begin{aligned}
&\int_\Omega \boldsymbol{B}^T\boldsymbol{\sigma}\,\mathrm{d}\Omega = \int_{\Gamma_u} \boldsymbol{N}^T\bar{\boldsymbol{t}}\,\mathrm{d}\Gamma \\
&\int_\Omega \left(\boldsymbol{\Psi} - \boldsymbol{\Psi}_I\right)\boldsymbol{B}^T\boldsymbol{\sigma}\,\mathrm{d}\Omega + 2\int_{\Gamma_d} \boldsymbol{N}^T\boldsymbol{t}\,\mathrm{d}\Gamma = \int_{\Gamma_u} \left(\boldsymbol{\Psi} - \boldsymbol{\Psi}_I\right)\boldsymbol{N}^T\bar{\boldsymbol{t}}\,\mathrm{d}\Gamma
\end{aligned} \tag{4.19}$$

with the strain-nodal displacement matrix $\boldsymbol{B}$. The linearized equations of the total system are

$$\begin{bmatrix} \boldsymbol{K}_{aa} & \boldsymbol{K}_{ab} \\ \boldsymbol{K}_{ba} & \boldsymbol{K}_{bb} \end{bmatrix}\begin{bmatrix} \mathrm{d}\boldsymbol{a} \\ \mathrm{d}\boldsymbol{b} \end{bmatrix} = \begin{bmatrix} \boldsymbol{f}_a^{ext} \\ \boldsymbol{f}_b^{ext} \end{bmatrix} - \begin{bmatrix} \boldsymbol{f}_a^{int} \\ \boldsymbol{f}_b^{int} \end{bmatrix} \tag{4.20}$$

with the blocks of the global stiffness matrix $\boldsymbol{K}$ defined as

$$\begin{aligned} \boldsymbol{K}_{aa} &= \int_{\Omega} \boldsymbol{B}^T \boldsymbol{D}\boldsymbol{B}\,\mathrm{d}\Omega & \boldsymbol{K}_{ab} &= \int_{\Omega} \boldsymbol{B}^T \boldsymbol{D}\boldsymbol{B}\left(\boldsymbol{\Psi}-\boldsymbol{\Psi}_I\right)\mathrm{d}\Omega \\ \boldsymbol{K}_{ba} &= \int_{\Omega} \left(\boldsymbol{\Psi}-\boldsymbol{\Psi}_I\right)\boldsymbol{B}^T \boldsymbol{D}\boldsymbol{B}\,\mathrm{d}\Omega & \boldsymbol{K}_{bb} &= \int_{\Omega} \left(\boldsymbol{\Psi}-\boldsymbol{\Psi}_I\right)\boldsymbol{B}^T \boldsymbol{D}\boldsymbol{B}\left(\boldsymbol{\Psi}-\boldsymbol{\Psi}_I\right)\mathrm{d}\Omega + 4\int_{\Gamma_d} \boldsymbol{N}^T \boldsymbol{T}\boldsymbol{N}\,\mathrm{d}\Gamma \end{aligned}, \tag{4.21}$$

where $\boldsymbol{T}$ is the stiffness matrix at the discontinuity. The force vectors are equal to

$$\begin{aligned} f_a^{ext} &= \int_{\Gamma_u} \boldsymbol{N}^T \bar{\boldsymbol{t}}\,\mathrm{d}\Gamma & f_a^{int} &= \int_{\Omega} \boldsymbol{B}^T \boldsymbol{\sigma}\,\mathrm{d}\Omega \\ f_b^{ext} &= \int_{\Gamma_u} \left(\boldsymbol{\Psi}-\boldsymbol{\Psi}_I\right)\boldsymbol{N}^T \bar{\boldsymbol{t}}\,\mathrm{d}\Gamma & f_b^{int} &= \int_{\Omega} \left(\boldsymbol{\Psi}-\boldsymbol{\Psi}_I\right)\boldsymbol{B}^T \boldsymbol{\sigma}\,\mathrm{d}\Omega + 2\int_{\Gamma_d} \boldsymbol{N}^T t\,\mathrm{d}\Gamma \end{aligned}. \tag{4.22}$$

In un-cracked continuum, usually a linear elastic constitutive law between stresses and strains is assumed under tension. To activate a crack, the Rankine condition has to be fulfilled at least in one integration point in the element at the front of the crack tip

$$max\left\{\sigma_1, \sigma_2, \sigma_3\right\} > f_t, \tag{4.23}$$

where σ_i are the principal stresses and f_t is the tensile strength. This inequality can be also verified at the crack tip directly (Mariani and Perego 2003). A very important issue is a determination of the crack propagation direction. If this direction is known in advance, it can be assumed (fixed) directly. Otherwise a special criterion has to be used. The most popular criterion assumes that the direction of the crack extension is perpendicular to the direction of the maximum principal stress. To smooth the stress field around the crack tip, non-local stresses σ^* instead of local values can be taken to determine the crack direction (Wells and Sluys 2001)

$$\boldsymbol{\sigma}^* = \int_V \boldsymbol{\sigma}\, w\,\mathrm{d}V, \tag{4.24}$$

where the domain V is a semicircle at the front of the crack tip and a weight function w is defined as

$$w = \frac{1}{\left(2\pi\right)^{3/2} l^3} \exp\left(-\frac{r^2}{2l^2}\right). \tag{4.25}$$

Here the length l is the averaging length (usually equal to 3 times the average element size) and r denotes the distance between the integration point and crack tip. This operation does not introduce non-locality connected to material microstructure into the model. Mariani and Perego (2003) used higher order

polynomials for a better description of the stress state (and also the displacement state) around the crack tip. Stresses in the crack tip were determined using an interpolation of nodal values. Oliver et al. (2004) formulated a global tracking algorithm, where propagation directions of cracks were determined globally by solving a stationary anisotropic heat conduction type problem. Moes and Belytschko (2002) assumed that cohesive tractions had no influence on the crack propagation direction and used the maximum circumferential stress criterion from Linear Elastic Fracture Mechanics (LEFM). Another important item of the formulation is a discrete cohesive law which links tractions $\boldsymbol{t}$ with displacement jumps $[[u]]$ at a discontinuity. The simplest one assumes the following format of the loading function (Wells and Sluys 2001)

$$f\left([[u_n]],\kappa\right) = [[u_n]] - \kappa \tag{4.26}$$

with the history parameter κ equal to the maximum value of the displacement jump $[[u_n]]$ achieved during loading. Softening of the normal component of the traction vector can be described using an exponential

$$t_n = f_t \exp\left(-\frac{f_t\,\kappa}{G_f}\right) \tag{4.27}$$

or a linear relationship

$$t_n = f_t\left(1-\frac{\kappa}{\kappa_u}\right), \qquad \kappa_u = \frac{2\,G_f}{f_t}, \tag{4.28}$$

where G_f denotes the fracture energy. During unloading, the secant stiffness is used with a return to the origin (damage format). In a compressive regime, a penalty elastic stiffness matrix is assumed. In a tangent direction, a linear relationship between a displacement jump and traction is defined with the stiffness T_s. Similar constitutive models were used by Remmers at al. (2003) and Mergheim et al. (2005). Alternatively, formulations based on effective displacements described in Chapter 4.1 may be used (Mariani and Perego 2003, Comi and Mariani 2007). Note that the cohesive crack formulation with the coefficient η=0 (Eq. 4.1) is equivalent with the discontinuity model described above, if the stiffness T_s=0. To overcome convergence problems in situations when $[[u_n]]$ changes its sign, Cox (2009) modified a linear softening curve in normal direction as

$$t_n = f_t\left(1-\frac{\kappa}{\kappa_u}\right)\left(1-\exp\left(-d_f\,\frac{\kappa}{\kappa_u}\right)\right), \tag{4.29}$$

where d_f is a drop factor. With increasing the value of d_f, the influence of the second term diminishes. The same modification was applied to an exponential softening curve.

The inclusion of enriched displacements $\boldsymbol{b}$ requires several modifications in the standard FE code. The final number of extra degrees of freedom $\boldsymbol{b}$ is unknown at the beginning and it may grow during calculations. Therefore special techniques are required to handle the extra data. If an essential boundary condition has been specified at a node with enriched degrees of freedom, the additional condition b=0 has to be added at this node. A new crack segment can be defined in the converged configuration only. After defining a new segment, a current increment has to be restarted. Moreover, nodes that share the edge with a crack tip may not be enriched. A definition of the crack segment geometry obeys the following rules:

- a new crack segment is defined from one element side to another one (a crack tip cannot be placed inside elements),
- segment end points cannot be placed at element vertices,
- a crack segment is straight inside one element,
- a crack is continuous across elements and adjacent segments share the same point.

To avoid placing cracks at element's vertices, three minimal distances are declared (Fig. 4.4):

- minimum distance between the vertex and crack segment $v_{\min}$,
- minimum distance between the vertex and crack segment end point along the side $l_{\min}$,
- minimum distance between the triangle side not touched by a discontinuity and the crack segment end point $s_{\min}$.

With the same values of $v_{\min}$ and $l_{\min}$, the first condition is stronger, since it takes into account also the distance between the vertex and segment. Finally, a new scheme for calculating strains, stresses, internal forces and stiffness in a cracked

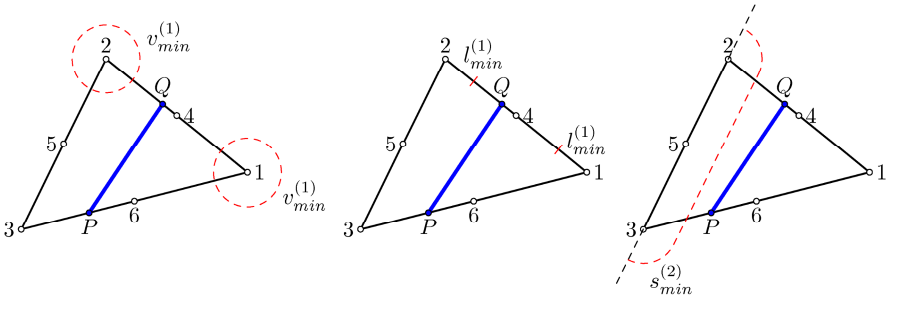

Fig. 4.4 Minimal distances between crack segment and triangle vertices/sides

element is required. Due to an arbitrary location of a discontinuity segment inside an element, new coordinates of integration points have to be defined. To determine these coordinates a sub-division algorithm is proposed. The triangle sub-region is divided into 3 triangles and quad sub-region into 4 triangles. In each triangle, 3 integration points are defined. In total, a numerical integration requires 21 integration points in the bulk and 2 points at the discontinuity (Wells and Sluys 2001, Bobiński and Brinkgreve 2010).

References

Bažant, Z., Jirásek, M.: Nonlocal integral formulations of plasticity and damage: survey of progress. Journal of Engineering Mechanics 128(11), 1119–1149 (2002)

Belytschko, T., Black, T.: Elastic crack growth in finite elements with minimal remeshing. International Journal for Numerical Methods in Engineering 45(5), 601–620 (1999)

Belytschko, T., Moes, N., Usui, S., Parimi, C.: Arbitrary discontinuities in finite elements. International Journal for Numerical Methods in Engineering 50(4), 993–1013 (2001)

Bobiński, J., Brinkgreve, R.: Objective determination of failure mechanisms in geomechanics, STW DCB.6368 Report, TU Delft (2010)

Camacho, G.T., Ortiz, M.: Computational modelling of impact damage in brittle materials. International Journal of Solids and Structures 33(20-22), 2899–2938 (1996)

Cazes, F., Coret, M., Combescure, A., Gravouil, A.: A thermodynamic method for the construction of a cohesive law from a nonlocal damage model. International Journal of Solids and Structures 46(6), 1476–1490 (2009)

Chandra, N., Li, H., Shet, C., Ghonem, H.: Some issues in the application of cohesive zone models for metal-ceramic interfaces. International Journal of Solids and Structures 39(10), 2827–2855 (2002)

Comi, C., Mariani, S.: Extended finite element simulation of quasi-brittle fracture in functionally graded materials. Computer Methods in Applied Mechanics and Engineering 196(41-44), 4013–4026 (2007)

Cox, J.V.: An extended finite element method with analytical enrichment for cohesive crack modelling. International Journal for Numerical Methods in Engineering 78(1), 48–83 (2009)

Daux, C., Moes, N., Dolbow, J., Sukumar, N., Belytschko, T.: Arbitrary branched and intersecting cracks with the extended finite element method. International Journal for Numerical Methods in Engineering 48(12), 1741–1760 (2000)

De Borst, T., Remmers, J.J.C.: Computational modelling of delamination. Composites Science and Technology 66(6), 713–722 (2006)

De Lorenzis, L., Zavarise, G.: Cohesive zone modeling of interfacial stresses in plated beams. International Journal of Solids and Structures 46(24), 4181–4191 (2009)

Dugdale, D.S.: Yielding of steel sheers containing slits. Journal of Mechanics and Physics of Solids 8(2), 100–108 (1960)

Gálvez, J.C., Červenka, J., Cendón, D.A., Saouma, V.: A discrete crack approach to normal/shear cracking of concrete. Cement and Concrete Research 32(10), 1567–1585 (2002)

Hansbo, A., Hansbo, P.: A finite element method for the simulation of strong and weak discontinuities in solid mechanics. Computer Methods in Applied Mechanics and Engineering 193(33-35), 3523–3540 (2004)

Hillerborg, A., Modeer, M., Peterson, P.E.: Analysis of crack propagation and crack growth in concrete by means of fracture mechanics and finite elements. Cement and Concrete Research 6(6), 773–782 (1976)

Mariani, S., Perego, U.: Extended finite element method for quasi-brittle fracture. International Journal for Numerical Methods in Engineering 58(1), 103–126 (2003)

Melenk, J.M., Babuška, I.: The partition of unity finite element method: basic theory and applications. Computer Methods in Applied Mechanics and Engineering 139(1-4), 289–314 (1996)

Mergheim, J., Kuhl, E., Steinman, P.: A finite element method for the computational modelling of cohesive cracks. International Journal for Numerical Methods in Engineering 63(2), 276–289 (2005)

Moës, N., Belytschko, T.: A finite element method for crack growth without remeshing. International Journal for Numerical Methods in Engineering 46(1), 131–150 (1999)

Moës, N., Belytschko, T.: Extended finite element method for cohesive crack growth. Engineering Fracture Mechanics 69(7), 813–833 (2002)

Needleman, A.: A continuum model for void nucleation by inclusion debonding. Journal of Applied Mechanics 54(3), 525–531 (1987)

Oliver, J., Huespe, A.E., Samaniego, E., Chaves, E.W.: Continuum approach to the numerical simulation of material failure in concrete. International Journal for Numerical and Analytical Methods in Geomechanics 28(7-8), 609–632 (2004)

Omiya, M., Kishimoto, K.: Damage-based cohesive zone model for rate-dependent interfacial fracture. International Journal of Damage Mechanics 19(4), 397–420 (2010)

Ortiz, M., Pandolfi, A.: Finite-deformation irreversible cohesive elements for three-dimensional crack-propagation analysis. International Journal for Numerical Methods in Engineering 44(9), 1267–1282 (1999)

Rabczuk, T., Zi, G., Gerstenberger, A., Wall, W.A.: A new crack tip element for the phantom-node method with arbitrary cohesive cracks. International Journal for Numerical Methods in Engineering 75(5), 577–599 (2008)

Remmers, J.J.C., de Borst, R., Needleman, A.: A cohesive segments method for the simulation of crack growth. Computational Mechanics 31(1-2), 69–77 (2003)

Samaniego, E., Belytschko, T.: Continuum-discontin0uum modelling of shear bands. International Journal for Numerical Methods in Engineering 63(13), 1857–1872 (2005)

Samimi, M., van Dommelen, J.A.W., Geers, M.G.D.: An enriched cohesive zone model for delamination in brittle interfaces. International Journal for Numerical Methods in Engineering 80(5), 609–630 (2009)

Scheider, I., Brocks, W.: Simulation of cup-cone fracture using the cohesive mode. Engineering Fracture Mechanics 70(14), 1943–1961 (2003)

Song, J.-H., Areias, P.M.A., Belytschko, T.: A method for dynamic crack and shear zone propagation with phantom nodes. International Journal for Numerical Methods in Engineering 67(6), 868–893 (2006)

Sukumar, N., Moës, N., Belytschko, T., Moran, B.: Extended finite element method for three-dimensional crack modelling. International Journal for Numerical Methods in Engineering 48(11), 1549–1570 (2000)

Wells, G.: Discontinuous modelling of strain localisation and failure. PhD Thesis, TU Delft (2001)

Wells, G.N., Sluys, L.J.: A new method for modelling cohesive cracks using finite elements. International Journal for Numerical Methods in Engineering 50(12), 2667–2682 (2001)

Yang, Z., Xu, X.F.: A heterogeneous cohesive model for quasi-brittle materials considering spatially varying random fracture properties. Computer Methods in Applied Mechanics and Engineering 197(45-48), 4027–4039 (2008)

Zhou, F., Molinari, J.F.: Dynamic crack propagation with cohesive elements: a methodology to address mesh dependency. International Journal for Numerical Methods in Engineering 59(1), 1–24 (2004)

Zi, G., Belytschko, T.: New crack-tip elements for XFEM and applications to cohesive cracks. International Journal for Numerical Methods in Engineering 57(15), 2221–2240 (2003)